Title

Intron 1–Mediated Regulation of EGFR Expression in EGFR-Dependent Malignancies Is Mediated by AP-1 and BET Proteins

Journal

Molecular Cancer Research, 17(11)

ISSN

1541-7786

Authors

Jameson, Nathan M
Ma, Jianhui
Benitez, Jorge
et al.

Publication Date

2019-11-01

DOI

10.1158/1541-7786.mcr-19-0747

Peer reviewed

HHS Public Access

Author manuscript

Mol Cancer Res. Author manuscript; available in PMC 2020 May 01.

Published in final edited form as:

Mol Cancer Res. 2019 November ; 17(11): 2208–2220. doi:10.1158/1541-7786.MCR-19-0747.

Intron 1-Mediated Regulation of *EGFR* Expression In EGFR-Dependent Malignancies is Mediated by AP-1 and BET Proteins

Nathan M. Jameson[1], **Jianhui Ma**[1,5], **Jorge Benitez**[1,4], **Alejandro Izurieta**[1], **Jee Yun Han**[3], **Robert Mendez**[3], **Alison Parisian**[1], **Frank Furnari**[1,2,*]

[1]Ludwig Cancer Research, San Diego Branch, University of California at San Diego, 9500 Gilman Drive, La Jolla, CA 92093-0660, USA

[2]The Department of Pathology, University of California San Diego, La Jolla, CA 92093, USA

[3]Center for Epigenomics, University of California at San Diego, 9500 Gilman Drive, La Jolla, CA 92093-0660, USA

[4]Celgene Corporation, 10300 Campus Point Drive Suite 100, San Diego, CA, 92121, USA

[5]Zeno Pharmaceuticals, 10835 Rd to the Cure #205, San Diego, CA 92121, USA

Abstract

The epidermal growth factor receptor (EGFR) is overexpressed in numerous solid tumors and is the subject of extensive therapeutic efforts. Much of the research on EGFR is focused on protein dynamics and downstream signaling, however few studies have explored its transcriptional regulation. Here, we identified two enhancers (CE1 and CE2) present within the first intron of the *EGFR* gene in models of glioblastoma (GBM) and head and neck squamous cell carcinoma (HNSCC). CE1 and CE2 contain open chromatin and H3K27Ac histone marks, enhance transcription in reporter assays, and interact with the *EGFR* promoter. Enhancer genetic deletion by CRISPR/Cas9 significantly reduces *EGFR* transcript levels, with double deletion exercising an additive effect. Targeted repression of CE1 and CE2 by dCas9-KRAB demonstrates repression of transcription similar to that of genomic deletion. We identify AP-1 transcription factor family members in concert with BET bromodomain proteins as modulators of CE1 and CE2 activity in HNSCC and GBM through *de novo* motif identification and validate their presence. Genetic inhibition of AP-1 or pharmacologic disruption of BET/AP-1 binding results in downregulated EGFR protein and transcript levels, confirming a role for these factors in CE1 and CE2. Our results identify and characterize these novel enhancers, shedding light on the role that epigenetic mechanisms play in regulating *EGFR* transcription in EGFR-dependent cancers.

Implications: We identify critical constituent enhancers present in the first intron of the *EGFR* gene, and provide rationale for therapeutic targeting of *EGFR* intron 1 enhancers through perturbation of AP-1 and BET in EGFR-positive malignancies.

Corresponding Author: Frank Furnari, Ludwig Institute for Cancer Research, San Diego Branch, University of California at San Diego, 9500 Gilman Drive, CMME #3020, La Jolla, CA 92093-0660, USA, Phone: 858-534-7819, Fax: 858-534-7750, ffurnari@ucsd.edu.

Conflicts of Interest: The authors declare no conflicts of interest.

Keywords

Enhancer; intron-1; *EGFR*; CRISPR/Cas9; AP-1

Introduction

Mammalian cells contain thousands of transcriptional control elements known as enhancers responsible for the regulation of gene expression (1). Enhancers contain open chromatin (2) and are marked by specific chromatin modifications, including mono-methylation of histone H3 at lysine 4 (H3K4me1) and acetylation of histone 3 at lysine 27 (H3K27Ac) (3). Active enhancers are typically identified by a specific enrichment of H3K27Ac (4) and contain high levels of enhancer-associated transcription factors (TF's) (5) that are often cancer-specific (6). The activator protein-1 (AP-1) family of oncogenic transcription factors activates transcription of different genes through homo- and hetero-dimers of Jun, Fos, and ATF family members (7) and has been shown to be critical for maintenance of GBM transcriptional heterogeneity (8). These factors bind to and modulate enhancer activity in combination with other chromatin associated proteins including BRD4 (9,10), the YAP/TAZ/TEAD complex (11,12), and the SWI/SNF (BAF) complex (13).

The epidermal growth factor receptor (EGFR) is a transmembrane tyrosine kinase whose downstream signaling pathways modulate a wide range of cellular activities, including growth, migration, and survival (14). EGFR is frequently overexpressed in a variety of cancer types, including cancers of the head and neck (HNSCC) and glioblastoma (GBM) (15). Over expression of EGFR is detectable in as much as 84% of HNSCC tumors, with mutation and/or amplification occurring in approximately 31% of these tumors (16), suggesting high EGFR protein levels are driven by transcriptional control mechanisms in HNSCC. GBM possesses a stronger correlation between *EGFR* copy number and expression, with mutation and/or amplification occurring in approximately 46% of GBM, over 90% of which overexpress the protein (17). Recent large-scale analysis of cancer epigenomes identified a significant relationship between somatic copy number alterations (SCNA's) and enhancer expression, with the most significant increases in enhancer expression occurring in tumors which have high aneuploidy and high mutation-load (18). HNSCC and GBM have high SCNA frequency (19) and a high frequency of *EGFR* gene alterations (20), indicating epigenome hyperactivity may play a role in overexpression of *EGFR*.

In spite of the prevalence of EGFR dependency in solid tumors, few studies have attempted to elucidate the mechanisms of transcriptional control of the gene. Early studies identified *cis*-acting elements which may regulate *EGFR* including CA dinucleotide repeats (21), intron 1 DNase I hypersensitive sites (22), and cooperative promoter-upstream and intron 1 enhancers (23). Lack of utilization of next generation sequencing (NGS) techniques limit the scope of these studies and argued for a larger breadth of analysis. Recently, EGFR super enhancers were identified in various cancer types including cervical, glioma, and lung (8,10,24–26), however systematic mapping of these super enhancers was lacking. The increased interest in enhancer-mediated expression of EGFR strongly argues for a clearer

understanding of the regions critical for enhancer function at *EGFR* and the transcription factors which mediate these effects.

In this study we interrogated the transcriptional regulation control of the *EGFR* locus. We utilized cell line models of solid tumors which commonly overexpress EGFR to identify the *cis*- and *trans*- acting factors involved in the transcriptional control of the *EGFR* gene and identified two critical constituent enhancers located within intron 1 of *EGFR*. We characterized these enhancers by mapping their domains with luciferase reporter assays, chromatin interaction assays, and CRISPR/Cas9-mediated genetic perturbation. Finally, genome-wide motif analysis implicated AP-1 TF and BET (Bromodomain and Extraterminal domain) protein family members whose presence and activity in *EGFR* intron 1 were further functionally validated. The results revealed that two constituent enhancers regulate *EGFR* transcriptional control, proposing an epigenetic regulation of the *EGFR* gene in cancer.

Materials and Methods

Cell Culture.

GBM cell lines U87 (RRID:CVCL_0022), T98G (RRID:CVCL_0556), LN229 (RRID:CVCL_0393) were purchased from ATCC. LNZ308 (RRID:CVCL_0394) was provided by Dr. Erwin Van Meir (Emory University, Atlanta, GA). SF767 (RRID:CVCL_6950) was provided by Dr. Mitch Berger (UCSF Brain Tumor Center, San Francisco, CA). Head and neck cell lines HN12 (RRID:CVCL_5518), Cal27 (RRID:CVCL_1107) and Detroit562 (RRID:CVCL_1171) (provided by Dr. Silvio Gutkind, UCSD Moores Cancer Center, San Diego, CA) were maintained in DMEM (Hyclone, #SH30022.01) supplemented with 10% fetal bovine serum (Atlanta Biologicals, #S12450) and 1% penicillin-streptomycin (Gibco, #15140-122) and grown as adherent cultures. GBM neurosphere cell lines GSC23 (RRID:CVCL_DR59, Dr. Fred Lang, University of Texas MD Anderson Cancer Center, Houston, TX) and TS576 (Dr. Cameron Brennan, Memorial Sloan Kettering Cancer Center, New York, NY) were maintained in DMEM/F12 (Gibco, #11320-033) supplemented with B27 supplement (Gibco, #12504-044) and 1% penicillin-streptomycin and grown in suspension. Mycoplasma testing was performed with the PlasmoTest kit (InvivoGen, #rep-pt1) and found to be negative. All experiments are performed within 10 passages of the original frozen stock or post-manipulation.

Luciferase reporter assays.

DNA fragments tested in the luciferase reporter assay were cloned from human genomic DNA (Promega, #G3041). PCR products were cloned downstream of firefly luciferase in the pGL4.24 minimal promoter vector (Promega, #E8421) using the SalI (NEB, #R3138S) site. Constructs were sequence confirmed by Sanger sequencing using the pGL4.24-R primer. pMIEG3-JunDN (RRID: Addgene_40350) and 3xAP1pGL3 (RRID:Addgene_40342) were gifts from Alexander Dent. pMIEG3-Empty was created by removing the JunDN sequence by EcoRI digestion. For each transfection reaction, 100ng control plasmid expressing *Renilla* luciferase (Promega, #E2241) and 1μg Firefly luciferase construct were co-transfected with Lipofectamine 2000 (ThermoFisher, #11668030) into 2 x 10^5 cells in a 12-

well plate well. After 24 hours, cells were collected in 1X PLB. Luciferase activity was measured by the Dual-Luciferase Reporter Assay System (Promega, #E1910) on a Tecan Spark 10M with injection control. Transfection efficiency was controlled for by dividing Firefly luminescence by *Renilla* luminescence, and final activity was normalized to a negative control.

Quantitative real-time PCR.

RNA was extracted with the RNeasy Plus kit (Qiagen, #74134) according to the manufacturer's instructions. Reverse transcription of mRNA was performed using 1μg RNA with the iScript Reverse Transcription Supermix (BioRad, #1708841). For real-time PCR analysis, 5μl of cDNA (50ng of starting RNA) was amplified per reaction using the iTaq Universal SYBR Green Supermix (Bio-Rad, #1725124) and the Bio-Rad CFX96 qPCR system.

Chromatin conformation capture (3C).

The experiment was performed as described (27) with the following modifications. Nuclei were treated with 1000U EcoRI (NEB, #R3101S) at 37°C overnight. 100U T4 enzyme (NEB, #M0202S) was added to digested nuclei and incubated at 16°C for 4 hours. Another 100U T4 enzyme was added and nuclei were incubated with rotation at 4°C overnight. 150ng of ligated DNA was quantified in triplicate by TaqMan real-time PCR using the PrimeTime Gene Expression Supermix (IDT, #1055772). Control 3C template was generated by using two bacterial artificial chromosomes (BACs) encompassing the entire *EGFR* gene, RP11-159M24 and RP11-148P17, were purchased from the Children's Hospital Oakland Research Institute (CHORI). Equimolar of the two BACs were digested with EcoRI and ligated. The ligation product from BAC control was used for normalization. The relative interaction frequency was calculated as: $2^{Ct\ (BAC)-Ct\ (3C)}$.

Guide RNA design.

Guide RNAs were designed using the MIT CRISPR Design website (http://crispr.mit.edu). To minimize potential off-target effects of guides, only high-score guide RNAs (score >80) were used. Guide RNA's were annealed and diluted 1:200 in ddH2O and used for downstream applications.

CRISPR/Cas9-mediated genomic deletion.

Guide RNAs were cloned into pX330-BFP (from Dr. Tim Fenton) for upstream guides or pX458-GFP (Addgene, Plasmid #48138) for downstream guides. Products were sequence verified by Sanger sequencing with the hU6-F primer. Constructs were co-transfected with Lipofectamine 3000 (ThermoFisher, #L3000015) into 4.5×10^5 cells in a 6-well plate. After 24 hours cells were collected and the top 1% of BFP+/GFP+ cells were sorted using the SH800S Cell Sorter (Sony Biotechnology). Single cells were plated in 96 well plates and grown for 2-3 weeks. Single clones were screened using PCR, and a minimum of 2 homozygous clones were mixed at equal ratios and used for downstream analysis.

Enhancer silencing by dCas9-KRAB.

SF767 and HN12 cells were transduced with Lenti-dCas9-KRAB-blast (from Dr. Paul Mischel) and selected with 10μg/ml blasticidin (Gibco, #A1113903) for 72 hours post transduction. Guide RNAs were cloned into the lentiGuide-Puro vector (Addgene, Plasmid #52963) and transformed into Stbl3 bacteria. Constructs were confirmed by Sanger sequencing using the hU6-F primer. Constructs were transduced individually into cells expressing dCas9-KRAB and selected with 1μg/ml puromycin. After assessing EGFR transcript levels by RT-qPCR, one highly effective CE1 guide-expressing cell line was selected for double gRNA expression and transduced with the complementary CE2 guide.

Cell growth analysis.

$5x10^2$ HN12, U87, or Cal27 cells or $1x10^4$ SF767 cells were seeded in 5 replicate black, clear bottom 96 well plate in 6 replicate wells in complete media. After 24 hours, complete media was removed and 100μl of 10μg/ml blasticidin and 1μg/ml puromycin in DMEM + 0.5% FBS was added to each well. Baseline luminescence was measured at day 1 with the ATPlite 1step Luminescence Assay System (PerkinElmer, #6016731) on a Tecan Spark 10M. Luminescence measurements were obtained at every other day for 9 days and plotted using GraphPad Prism.

Subcutaneous tumor growth.

$1x10^6$ HN12 parental (n = 5) or $CE1^{-/-}CE2^{-/-}$ (n = 4) cells were injected into the right flank of nude mice. Tumors were measured by caliper every 4 days until visible tumors formed and then measured every day until the appearance of necrosis or the volume reached $500mm^3$. The animal studies are approved by UCSD IACUC according to the NIH guidelines.

siRNA transfection.

$1x10^5$ SF767 or $5x10^5$ HN12 cells were seeded in 12 well plates and grown overnight. siRNA's were transfected into each well with Lipofectamine 2000 in serum free and antibiotic free DMEM. Media was changed to complete media 6 hours later. Samples were collected in SDS sample buffer 48-72 hours later. siRNA's used for this study include BRD2 (Ambion, #s12070), BRD3 (Ambion, #s15544), BRD4 (Ambion, #s23902), and scramble control (Invitrogen, #12935-300).

JQ1 Treatment.

SF767 or HN12 cells were treated with 0.5μM JQ1 dissolved in DMSO (MedChemExpress, #HY-13030) for 24 hours. Vehicle control samples were treated with equal volume DMSO for 24 hours.

Western blotting.

Protein samples were collected in SDS sample buffer, separated using gel electrophoresis and transferred via wet transfer onto a PVDF membrane. The membrane was blocked with 5% milk in TBST and probed with primary antibodies at 1:1000 dilution overnight at 4°C and secondary HRP antibodies at 1:2000 for 1 hour at RT. Signal was assessed via

chemiluminescence with the SuperSignal West Pico PLUS substrate (ThermoFisher, #34580) and visualized on a ChemiDoc MP system (Bio-Rad). Anti-Cas9 antibody (Cell Signaling, #14697), anti-β-actin (Sigma, #A3854), anti-c-Jun (Cell Signaling, #9165S), anti-c-Fos (Santa Cruz Biotechnology, #sc-52), anti-HA-HRP (Santa Cruz Biotechnology, #sc-805), anti-BRD4 (Active Motif, #39909), anti-BRD3 (Santa Cruz Biotechnology, #sc-515729), anti-BRD2 (Cell Signaling, #5848S), and c-Myc (Cell Signaling, #9402) and anti-EGFR (BD Biosciences, #610017) were used for analysis.

Chromatin immunoprecipitation.

Chromatin immunoprecipitation was performed as described previously (28) with the following modifications. Chromatin was sheared in diluted lysis buffer to 200-500bp using a Covaris M220 Focused-Ultrasonicator with the following parameters: 10 minutes, peak incident power 75, duty factor 10%, 200 cycles/burst. Antibodies for ChIP were obtained from commercially available sources: anti-H3K27Ac (Active Motif, #39133), anti-BRD4 (Active Motif, #39909), anti-c-Jun (Cell Signaling, #9165T), anti-c-Fos (Santa Cruz Biotechnology, #sc-166940), anti-BRD3 (Santa Cruz Biotechnology, #sc-515729), and anti-BRD2 (Cell Signaling, #5848S). 5% of the chromatin was not exposed to antibody and was used as control (input). For ChIP-qPCR analysis DNA quantity for each ChIP sample was normalized against input DNA. For ChIP-seq samples, after DNA purification ChIP-seq DNA libraries were prepared with either the TruSeq ChiP Library Prep Kit (Illumina, #IP-202-1012) or the Accel-NGS 2S Plus DNA Library kit (Swift Bioscience, #21024) and sequenced using 75 bp single-end sequencing on an Illumina Hi-seq 4000.

ATAC-seq.

Approximately 50,000 permeabilized nuclei were transposed using Tn5 transposase (Illumina, #FC-121-1030) as described previously (29). Libraries were amplified using NEBNext High-Fidelity 2X PCR Master Mix (NEB, #M0541) with primer extension at 72°C for 5 min, denaturation at 98°C for 30s, followed by 8 cycles of denaturation at 98°C for 10s, annealing at 63°C for 30s and extension at 72°C for 60s. Each library was size selected and sequenced on an Illumina NextSeq500 or HiSeq4000 to a depth of ≥ 20 million usable reads pairs. Sequencing runs that did not meet the read pair threshold were sequenced again, and all replicates were pooled for analysis. Tracks shown in figures 1A and supplemental figure 2 are pooled from two biological replicates.

Statistical Analysis.

Correlative statistical analysis was performed on the relationship between ChIP-seq read count data and relative luciferase expression, *EGFR* expression, or relative interaction frequency using Spearman's Rank-Order Correlation. Data from chromosomal interaction, CRISPR/Cas9 deletion, cell proliferation, and ChIP-qPCR enrichment were compared, and statistical analysis was performed using a Student's *t* test.

Oligo Sequences.

All DNA oligo (primer, gRNA) sequences are listed in Supplementary Table S2.

Data Access.

All raw and processed sequencing data generated in this study have been submitted to the NCBI Gene Expression Omnibus (GEO; http://www.ncbi.nlm.nih.gov/geo/) under accession number GSE128275. Accession numbers for publicly available data accessed are listed in Supplementary Table S1.

Results

EGFR Intron 1 Contains Open Chromatin Regions Containing Histone Marks Indicative of Enhancers

To gain further insight into the mechanisms responsible for *EGFR* transcriptional control in HNSCC and GBM we performed ChIP-seq and ATAC-seq in 7 GBM and 3 HNSCC cell lines with non-amplified *EGFR* copy numbers and varying levels of *EGFR* activation. Overlay of IGV tracks of all 10 cell lines showed conservation of H3K27Ac intensity and open chromatin throughout intron 1, indicating the presence of enhancers in these regions (Fig. 1A). Since super enhancers (SE) are defined as large clusters of transcriptional enhancers that drive expression of genes that define cell identity, and are often found at oncogenes (30) we identified SE's using the ROSE (Rank Ordering of Super-Enhancers) algorithm (6,31) (Supplementary Fig. 1A). Using this algorithm, we discovered cell-line specific SE's in the first intron of *EGFR*, many of which rank highly in several of our cell lines (Supplementary Fig. 1B). Interestingly, the location and size of these SE's varied and were dependent upon the local enrichment of H3K27Ac ChIP-seq signal.

To determine if presence of putative enhancers in *EGFR* intron 1 was predictive of *EGFR* expression we first measured *EGFR* transcript in each GBM and HNSCC cell line (Fig. 1B). Due to cell line-specific presence and location of predicted *EGFR* super enhancers, we used total number of intron-1 mapped H3K27ac ChIP-seq reads as a measure of enhancer presence and plotted these values against the fold change in *EGFR* expression. Analyzing the relationship by Spearman's correlation showed a highly significant correlation (Fig. 1C). Together, these results identify regions containing characteristics of SE's in the first intron of *EGFR* and suggests that presence of these putative enhancers is important for high levels of *EGFR* transcript.

Two Critical Constituent Enhancers Reside in the First Intron of EGFR

It has been reported previously that SE's are congregations of active constituent enhancers (CE) (32). To determine which CE's of the identified SE's are active, we segmented regions which exhibited highly conserved H3K27Ac ChIP-seq and ATAC-seq signals into 2kb segments (Supplemental Fig. 2). Each segment was then measured for enhancer activity by *in vitro* bioluminescence (Fig. 2A). Regions which exhibited conserved luciferase expression included 1, 3, and 16-19. Interestingly, activity of segments 8 and 9 were HNSCC specific, while segments 1 and 3 were more glioma specific. Segments 16-19 consistently enhanced luciferase activity in both tumor models. Combining H3K27Ac presence by ChIP-seq, open chromatin accessible regions by ATAC-seq, and functional activity as defined by our luciferase system in both tumor types, we define two distinct CE's. Specifically, we combined segments 1-3 into an approximately 6kb region which we have

termed Constituent Enhancer 1 (CE1), and combined segments 16-19 into an approximately 8kb region which we have termed Constituent Enhancer 2 (CE2) (Fig. 2A). CE1 and CE2 reside in regions of conserved high levels of H3K27Ac, however other segments do not have associated H3K27Ac enrichment. We hypothesized that the specific enrichment of H3K27Ac at an enhancer segment would correlate to luciferase expression in the matched cell line. Indeed, plotting the normalized luciferase intensity against the average H3K27Ac read intensity (Fig. 2B and 2C) reveals a highly significant relationship ($p < 0.001$, Spearman's correlation). These results define two conserved putative CE's within *EGFR* intron 1 and establish a relationship between histone acetylation at these regions and enhancer activity as measured by *in vitro* bioluminescence.

Significant Interactions Between CE1, CE2 and the EGFR Promoter

Enhancers typically make contact with one or more gene promoters through long-range interactions (30). To test if the predicted enhancer regions CE1 or CE2 interact with the *EGFR* promoter we performed a chromosome conformation capture (3C) assay. Primers were designed around the *EcoRI* sites in CE1 (F1 to F5) and CE2 (F6 to F10) and nearby the *EGFR* promoter (Fig. 3A). Since we hypothesized that an increased interaction frequency would correlate with increased transcript levels, we chose the cell lines with the highest *EGFR* expression levels in both tumor types (HN12/SF767) and compared them against a cell line with virtually no *EGFR* expression (TS576). Compared to TS576, in SF767 cells low levels of interaction with CE1 and CE2 were found; however, significantly stronger interactions were identified at F2 and F4 of CE1 and 4 out of 5 regions of CE2 in the HN12 cell line (Fig. 3B). These primers reside in highly acetylated regions in HN12 cells, thus we hypothesized there is a correlation between H3K27Ac intensity and interaction frequency. Correspondingly, we identified a significant correlation between H3K27Ac peak intensity and interaction frequency when comparing all three cell lines (Fig. 3C). Together, the data thus far indicates that CE1 and CE2 have characteristics ascribing them to active enhancers: surrounded by nucleosomes with high H3K27Ac, open chromatin, transcriptional enhancement, and interaction with a promoter.

Deletion of CE1 and CE2 by CRISPR/Cas9 Results in Reduced EGFR Expression

To directly assess if CE1 and CE2 were essential for *EGFR* expression, we used the CRISPR/Cas9 system to delete CE1 (hg 38, chr7: 55,060,994-55,066,815) and CE2 (hg38, chr7: 55,127,646-55,135,347). To test how enhancer loss effects cells with different *EGFR* expression levels we made these deletions in two GBM cell lines and two HNSCC cell lines which had either high (SF767, HN12) or low (U87, Cal27) relative *EGFR* expression. Single enhancer deletions were generated with a dual-guide deletion strategy (Fig. 4A) and the deletion was confirmed by genotyping PCR (Fig. 4B). Compared to parental cell lines, *EGFR* transcript and protein was significantly decreased in each deletion (Fig. 4C). In those cell lines which express EGFR highly, CE1 deletion provided the strongest knockdown of EGFR transcript and protein, however U87 had the strongest effect in the CE2 knockout cell line. Cell-type specific differences in transcript levels between CE1 and CE2 indicate there may be differential utilization of either CE1 or CE2 in different cell lines, possibly due to cell line specific expression of transcription factors critical for *EGFR* enhancer activity.

Previous studies have indicated partial redundant control of a gene by multiple CE's within a single SE (32). To evaluate if there was a compensatory effect on *EGFR* transcription by either CE1 or CE2, we performed a second round of CRISPR/Cas9 editing on the homozygous edited populations (Fig. 4D). Compared to parental cell lines, *EGFR* transcript levels were significantly decreased with loss of both enhancers (Fig. 4E). Notably, the amplitude of *EGFR* transcript loss was greater in $CE1^{-/-}$+$CE2^{-/-}$ when compared against $CE1^{-/-}$ or $CE2^{-/-}$ alone. EGFR transcript and protein loss corresponded to significant proliferation deficiencies in each cell line measured, notably most significantly in double deleted cell lines (Fig. 4F). In HN12 cells, this proliferation difference between parental and double knockout cells translates to a significant repression of tumor growth in a subcutaneous tumor model (Fig. 4G). Restoring EGFR protein by lentiviral transduction of wild-type EGFR in $CE1^{-/-}$+$CE2^{-/-}$ cells results in significant rescue of proliferation in HN12 cells (Fig. 4H). Incomplete rescue of growth in these cells indicates CE1 or CE2 may be enhancing other genes important for cell growth. Together, these results demonstrate both cell type-specific CE utilization as well as a cooperative relationship between the CE1 and CE2 whereby double enhancer deletion results in more significant deleterious effects than single deletions alone.

Repression of H3K27Ac by dCas9-KRAB Decreases EGFR Expression

To eliminate the possibility of structural variation being the root cause of *EGFR* expression-loss in CRISPR/Cas9 deleted clones, we hypothesized that histone de-acetylation would be sufficient for *EGFR* transcriptional repression. dCas9-KRAB is known to recruit endogenous chromatin modifying complexes to de-acetylate histones (33), therefore to test our hypothesis we targeted a nuclease deactivated Cas9 (dCas9) protein fused to the Krüppel-associated box (KRAB) domain of Kox1 (34) with four CE1 and five CE2 gRNAs in HN12 (Fig. 5A) and SF767 (Supplementary Fig. 3A) cell lines.

To ensure successful targeting of dCas9-KRAB we confirmed de-acetylation at the targeted regions. Compared to an enhancer off-target (O-T) gRNA, the targeting of dCas9-KRAB resulted in significant decreases in H3K27Ac in HN12 cells (Fig. 5B). Additionally, we measured *EGFR* transcript and protein levels and observed significant decreases in transcript in 80% (8/10) of enhancer-specific targeted regions (Fig. 5C). Interestingly, targeting CE2 had an overall stronger repressive effect on *EGFR* transcript levels, with repression by gRNA targeting CE2.4 achieving a greater than 3-fold decrease in expression. We performed double dCas9-KRAB repression by adding a second gRNA (CE1.4 + CE2.4) and observed the most significant decrease in *EGFR* transcript and protein levels, achieving an 8-fold decrease in RNA expression compared to the off-target gRNA (Fig. 5C). In SF767 cells, dCas9-KRAB was expressed to lower levels than that of HN12 (Supplementary Fig. 3A) and correspondingly we saw less significant reductions in H3K27Ac (Supplementary Fig. 3B). Importantly, we still saw significant repression of *EGFR* transcript levels in 50% (5/10) of enhancer-specific targeted regions in SF767 (Supplementary Fig. 3C). In these cells there was no observable preference for CE2, however the strongest repression was again observed by combining CE1.4 and CE2.4.

Finally, the effect of dCas9-KRAB-mediated *EGFR* repression on cell proliferation was assessed by ATPlite assay. At low (0.5%) serum, the relative proliferation of the indicated *EGFR*-repressed cells was significantly inhibited (Fig. 5D, Supplemental Fig. 3D). Importantly, cell lines with stronger *EGFR*-repression exhibited reduced proliferation over time. Reintroducing high levels of wild-type EGFR by lentiviral transduction resulted in a rescue of the proliferation ability of double knockdown cells. These results indicate that *EGFR* transcriptional changes in enhancer deleted regions (Fig. 4) are not due solely to structural alteration within the first intron. Moreover, these results demonstrate that loss of H3K27Ac at the identified *EGFR* enhancers is sufficient for significant decreases in EGFR protein and transcript levels and this reduction in EGFR is sufficient to reduce cell growth.

AP-1 Family Transcription Factors Bind to and Influence EGFR Intron 1 Enhancers

To identify transcription factors important for enhancer activity we further analyzed our H3K27Ac ChIP-seq and ATAC-seq data. To eliminate non-enhancer regulatory regions, we intersected ATAC-seq peaks with enhancer peaks from H3K27Ac and kept the TSS-distal (+/− 2.5kb) ATAC-seq peaks which mapped within an enhancer. Performing *de novo* motif analysis on these peaks in *EGFR* expressing cells (SF767 and HN12) identified an AP-1 transcription factor motif as the most significantly enriched motif (Supplemental Fig. 4A).

To validate the TF motifs identified *in silico*, we examined AP-1 family transcription factor ChIP-seq data deposited by the Encyclopedia of DNA Elements (ENCODE) consortium (Supplemental Table 1). Using this approach multiple c-Jun and c-Fos peaks were identified within the CE1 and CE2 of *EGFR* in HN12 and SF767 cells (Fig. 6A). Importantly, H3K27Ac ChIP-seq in HeLa-S3 and HUVEC also shows high levels of enhancer marks in the AP-1 marked regions (Supplemental Fig. 4B). For further analysis we chose c-Jun and c-Fos as the prototype AP-1 factors which form heterodimers that bind to the consensus 5'-TGA(C/G)TCA motif-3' (35). We validated and quantified c-Fos and c-Jun enrichment at the CE1 and CE2 regions in *EGFR* expressing (SF767 and HN12) and non-expressing (TS576) cells and identified significant fold enrichment of both factors in *EGFR* expressing cells (Fig. 6B). Additionally, we identified significantly increased binding of c-Fos at the CE1-AP1-3 and c-Jun in CE1-AP1.3 and CE2-AP1.4 sub-regions in HN12 cells indicating these regions may be important for the increased *EGFR* expression levels in these cells.

To validate the role of AP-1 transcription factors in *EGFR* transcription, we utilized a dominant-negative version of c-Jun (JunDN) (36). JunDN can dimerize with other AP-1 family members and bind DNA, however the transcriptional activation capability is eliminated. HN12 and U87 cells transduced with JunDN showed decreased EGFR protein levels, thus supporting a role for c-Jun heterodimers in the regulation of *EGFR* transcription (Fig. 6C, Supplemental Fig. 4C). Additionally, we detected a decrease in c-Jun levels when JunDN was present, likely due to autoregulation of the *Jun* promoter by c-Jun heterodimers (37). To confirm the effect of JunDN was due to reduced c-Jun heterodimer activity, we utilized a luciferase reporter containing a trimerized AP-1 binding motif. Luciferase reporter assays showed significant decreases in activity when JunDN is present compared to the empty vector control, confirming the reduced transcriptional activation potential of JunDN (Fig. 6D, Supplemental Fig. 4D). Taken together, these data suggest that AP-1 family

members are critical for fine-tuned regulation of *EGFR* expression and specifically bind to *EGFR* enhancer regions. Perturbation of this AP-1 transactivation effect by expression of a dominant negative results in a significant repression of c-Jun heterodimer targets including EGFR and c-Jun, confirming the role of this family of transcription factors in intron 1-mediated *EGFR* expression.

Treatment with JQ1 Reduces EGFR Expression by Modulation of TF Activity

Previous research from our lab has shown treatment of mice harboring GBM neurosphere PDX models with the BET protein inhibitor JQ1 significantly prolongs survival, and combination of JQ1 with anti-EGFR therapy further increases this effect (38). To determine if this effect of JQ1 is partially attributable to downregulation of *EGFR* transcription through BET proteins we treated HN12 and SF767 cells with JQ1 and measured the effects on *EGFR* expression. Interestingly, after 24 hours of 0.5μM JQ1 EGFR protein and transcript levels were decreased in both HN12 (Fig. 7A, 7B) and SF767 (Supplementary Fig. 5A, 5B) cell lines. Protein expression of BET proteins BRD2, BRD3 and BRD4 increased in response to JQ1, however protein level of the known BRD4 target c-Myc was downregulated (Fig. 7A).

BRD4 is known to co-occupy enhancers with AP-1 family members (9,10) and is enriched at enhancers (6), and BRD2/3 have been shown to bind to hyperacetylated regions and allow for the activity of RNA polymerase II (39). JQ1 is a pan-BET inhibitor (40) thus to determine if JQ1 treatment was affecting *EGFR* levels through reduced activity of select BET family members, we first looked at expression levels of BET proteins in our cell line panel and found their expression to be highly variable but present in most cell lines (Supplemental Fig. 5C). We then looked for evidence of binding of these factors to CE1 and CE2. Recent data in the liposarcoma cell line LPS141 (41) shows presence of H3K27Ac in CE1 and CE2, and has binding of BET family members BRD2, BRD3 and BRD4 in those regions (Supplemental Fig. 5D). To confirm binding of these factors in GBM and HNSCC and to interrogate their relationship with AP-1, we performed ChIP-qPCR for c-Fos, c-Jun, BRD2, BRD3, BRD4 and H3K27Ac at regions of open chromatin in CE1 and CE2. In HN12 cells, treatment with JQ1 significantly reduces occupancy of H3K27Ac at all measured regions, and significantly reduces binding of BET and AP-1 family transcription factors to CE1 and CE2 (Fig. 7C). Interestingly, in contrast to steady state (Fig. 6C) which suggests CE2-AP1.4 is a critical c-Fos and c-Jun binding site, treatment with JQ1 only affects binding of BRD4 at that region (Fig. 7C). In SF767 cells, significant reductions in TF occupancy were observed primarily in CE2, with only BRD4 showing a significant reduction in binding to CE1 (Supplemental Fig. 5E). Importantly, JQ1 treatment also impedes *EGFR* transcription by inhibiting the interaction between CE1/CE2 and the *EGFR* promoter as measured by 3C (Fig. 7D, Supplemental Fig. 5F).

To determine the specific BET protein critical for maintenance of *EGFR* expression we performed siRNA knockdowns of BRD2/¾ individually as well as in combination. In HN12 cells single knockdown of BRD2 or BRD4, but not BRD3, resulted in downregulation of EGFR protein. Complete loss of BRD2/¾ protein by combination siRNA treatment resulted in the strongest downregulation of EGFR protein (Fig. 7D). In SF767 cells single knockdown of BRD2 produced the strongest downregulation of EGFR protein

(Supplementary Fig. 5F), indicating BRD2 and BRD4 activity on EGFR expression may be cell type specific.

To further interrogate the relationship between EGFR, AP-1, and BET clinically we utilized H3K27Ac ChIP-seq and matched RNA-seq in 44 patient derived glioblastoma stem cells (GSCs) and 50 primary tumors (24). We organized these samples by their *EGFR* expression by RNA-seq and found that those tumors which have high *EGFR* also have high levels of H3K27Ac in intron 1 (Supplemental Fig. 6A). We then plotted *EGFR* RNA expression versus expression of *JUN, FOS, BRD2*, and *BRD4* and found significant correlations between expression of these transcription factors and *EGFR* levels (Supplemental Fig. 6B). Finally, to determine if the activity of the *EGFR* enhancers are tumor specific we compared expression of these genes between tumor and normal samples in the TCGA database (42) (Supplemental Fig. 6C). We found in GBM tumor samples transcript levels for *EGFR, FOS, JUN, BRD2*, and *BRD4* are significantly upregulated versus normal samples. In HNSCC tumor samples, transcript levels for *EGFR, BRD2*, and *BRD4* are significantly upregulated versus normal samples. Taken together these results implicate a role for BRD2 and BRD4 cooperating with AP-1, in the maintenance of *EGFR* expression in GBM and HNSCC.

Discussion

In this study we identify regions of epigenetic regulation within the first intron of the *EGFR* gene in GBM and HNSCC, characterizing DNA regions which are cell type specific in their H3K27Ac deposition, but contain conserved regions of open chromatin and histone acetylation within *EGFR*-expressing cells. These regions pass the threshold to be considered super enhancers and contain individual constituents which demonstrate functional attributes of active enhancers, including transcriptional enhancement in reporter assays, 3D interactions with the *EGFR* promoter, and negative regulation of their target gene when removed or repressed. We identify the presence and activity of AP-1 transcription factors in the CE1 and CE2, and when the activity of these transcription factors is eliminated significant effects are seen in expression of target genes including *EGFR* and *JUN*, indicating direct AP-1 dependency of these genes. Pharmacologic disruption of the transcription factor complexes at these enhancers has significant effects on *EGFR* expression, providing a mechanism by which this transcriptional control mechanism may be targeted. While identification of *EGFR* super enhancers in other tumor types has been published previously (8,10,24–26), this study provides significant advances in our understanding of the most critical *EGFR* enhancer regions by undertaking functional genomic and pharmacologic approaches to directly perturb their activity and demonstrating functional consequences on tumor cell proliferation both *in vitro* and *in vivo*.

Elevated EGFR is a well-established therapeutic target, however responses to EGFR tyrosine kinase inhibitors (TKI) are sporadic. The mechanisms behind resistance to EGFR TKI are unique to each tumor type, and secondary resistance mutations are common. In HNSCC, high *EGFR* copy numbers are statistically associated with cetuximab and gefitinib resistance (43), and although rare, kinase domain mutations may be associated with altered responses to EGFR inhibitors (44). In GBM, resistance mechanisms are less well understood with prevailing theories including intratumoral heterogeneity (45), *EGFR* amplified

extrachromosomal DNA (ecDNA) (46), and loss of *PTEN* (47). Another tumor type which has a high prevalence of *EGFR* overexpression is non-small cell lung cancer (NSCLC), the resistance mechanisms for which are largely kinase-domain mutations (48,49). With these challenges in mind, this study presents a kinase domain independent mechanism by which *EGFR* expression and activity can be prevented. Recent studies have shown targeted transcription factor blockade can overcome EGFR TKI resistance (50), thus this study presents an additional pathway which can be targeted alone or in combination with EGFR TKI's to treat *EGFR*-positive tumors. Further studies should interrogate the CE1 and CE2 in *EGFR*-mutated models, specifically in NSCLC where TKI-resistant *EGFR* mutations are present in as much as 63% of tumors (48).

This study focuses exclusively on non-amplified *EGFR*, however significant fractions of both HNSCC and GBM tumors have high copy numbers of the gene (16,51). In GBM, *EGFR* can be amplified both as a homogeneously staining region (HSR) or on ecDNA (46), both of which include the entire *EGFR* gene and surrounding regions. Amplified enhancer regions maintain their enhancer signatures (52) and focal amplifications of super enhancers have been shown to drive transcription (53). Because amplified enhancers have standard enhancer features, we hypothesize that targeting amplified *EGFR* directly (Fig. 5) or pharmacologically (Fig. 7) will have similar inhibitory effects. Future studies should explore this hypothesis to further broaden the clinical implications of targeting *EGFR* intron 1 enhancers.

In tumor types which frequently alter EGFR, structural variations (SV's) are common. One such SV, EGFR variant III (EGFRvIII), is an extracellular domain mutation which shows constitutive tyrosine kinase activity (54). The mutant receptor is highly tumor specific (55) and relatively common in GBM (51). EGFRvIII protein has been identified in other tumor types including HNSCC (56), although genomic deletion of exons 2-7 have not been detected. In GBM every incidence of EGFRvIII has unique genomic breakpoints within intron 1 and intron 8, removing exons 2-7 and large portions of intron 1 depending on breakpoint location, often including regions which we have identified as enhancers (57) (Fig. 1A). It is important to note the majority of identified *EGFRvIII* breakpoints occur nearer the 3' end of *EGFR* intron 1, often removing the region which we have identified as CE2 (57). Interestingly, in some of our cell line models the data indicates a more significant role for CE2 in interaction with the *EGFR* promoter by 3C (Fig. 3) and influence on the expression of *EGFR* by dCas9-KRAB (Fig. 5). In other models the utilization of each CE is either equal (Supplemental Fig. 3) or demonstrates a CE1 bias (Fig. 4C, HN12/SF767/Cal27). But, targeting both CE's always produces a combinatorial effect (Fig. 4, 5). These data demonstrate an intricate regulatory system that is cell type-specific and makes predicting the functional consequences of intron 1-loss on *EGFRvIII* expression difficult. Further research should interrogate directly how extent of intron 1-loss affects *EGFRvIII* through analysis of patient derived and/or CRISPR/Cas9-generated *EGFRvIII+* models.

Many potent oncogenes are associated with super enhancers, including *MYC* and *HER2* (30,58). These genes and others have been successfully targeted in cancers which express them by inhibiting the BET protein BRD4, a hallmark factor involved in super enhancer identity (6). The BET-bromodomain inhibitor JQ1 has been shown to inhibit BRD4 at super

enhancers (6) and additionally sensitizes *EGFR* amplified GBM (38) and HNSCC (59) cells to EGFR TKI. Our data suggests that this sensitization may also be due in part to JQ1-mediated inhibition of AP-1 and other BET proteins at *EGFR* intron 1 enhancers (Fig. 7). Although site-specific inhibition of TF binding is cell type dependent, whether targeting TF binding pharmacologically (Fig. 7A–D, Supplemental Fig. 5A–G) or through RNAi (Fig. 7E, Supplemental Fig. 5F), the effects on EGFR are consistently deleterious. These results support the global targeting of AP-1 and BET rather than site-specific repression (e.g. dCas9-KRAB). Additionally, our study shows significant reduction of EGFR protein and transcript after JQ1 treatment independent of gene expression (Fig. 7A–B, Supplemental Fig. 5A–B), indicating a broader effect of JQ1 on tumor models which express *EGFR* at varying levels. Indeed, *EGFR* transcript levels are reduced to similar levels in SF767 cells which express less *EGFR* and exhibit less significant TF occupancy differences in response to JQ1 treatment (Supplementary Fig. 5E). Further, clinical benefit for patients with EGFR-expressing GBMs is supported by the presence of super enhancers in EGFR-positive GSC and primary tumor samples (Supplemental Fig. 6A). These tumors exhibit positive correlations between critical TF expression and *EGFR* mRNA, and suggest limited off-target effects in the brain due to significant differences in TF expression between normal and tumor tissues (Supplemental Fig. 6B–C). These data combined further support the combination of EGFR TKI and JQ1 as treatment for EGFR-positive malignancies.

In conclusion we found that *EGFR* expression is maintained in part through presence and activity of critical enhancers present in intron 1 of the gene. Characterization of CE1 and CE2 in multiple cell line systems identified a novel role for BET transcriptional co-activators and AP-1 transcription factors in these enhancers, and provided the rationale for therapeutic targeting of EGFR through perturbation of BET and AP-1 in *EGFR*-positive malignancies.

Supplementary Material

Refer to Web version on PubMed Central for supplementary material.

Acknowledgments

We thank Dr. Bing Ren for sharing the ChIP protocol; Dr. Paul Mischel and Dr. Sudhir Chowdry for sharing the dCas9-KRAB-Blast and lentiGuide-Puro vectors; Dr. David Gorkin for advising on the ATAC-seq data generation and analysis; Dr. Silvio Gutkind for sharing the HNSCC cell lines; Dr. Roman Sasik for providing the ChIP-seq analysis pipeline.

Financial Support: This work was supported by grants from the NIH (NS080939) (to F.F.) and the UCSD Cancer Biology, Informatics & Omics Training Program (T32-CA067754-22) (to N.M.J.)

REFERENCES

1. Bulger M, Groudine M. Functional and mechanistic diversity of distal transcription enhancers. Cell. 2011;144:327–39. [PubMed: 21295696]
2. Thurman RE, Rynes E, Humbert R, Vierstra J, Maurano MT, Haugen E, et al. The accessible chromatin landscape of the human genome. Nature. 2012;489:75–82. [PubMed: 22955617]
3. Calo E, Wysocka J. Modification of enhancer chromatin: what, how, and why? Mol Cell. 2013;49:825–37. [PubMed: 23473601]

4. Creyghton MP, Cheng AW, Welstead GG, Kooistra T, Carey BW, Steine EJ, et al. Histone H3K27ac separates active from poised enhancers and predicts developmental state. Proc Natl Acad Sci U S A. 2010;107:21931–6. [PubMed: 21106759]
5. Ong C-T, Corces VG. Enhancer function: new insights into the regulation of tissue-specific gene expression. Nat Rev Genet. Nature Publishing Group; 2011;12:283–93.
6. Lovén J, Hoke HA, Lin CY, Lau A, Orlando DA, Vakoc CR, et al. Selective inhibition of tumor oncogenes by disruption of super-enhancers. Cell. 2013;153:320–34. [PubMed: 23582323]
7. Shaulian E, Karin M. AP-1 in cell proliferation and survival. Oncogene. 2001;20:2390–400. [PubMed: 11402335]
8. Chu T, Rice EJ, Booth GT, Salamanca HH, Wang Z, Core LJ, et al. Chromatin run-on and sequencing maps the transcriptional regulatory landscape of glioblastoma multiforme. Nat Genet. Nature Publishing Group; 2018;50:1553–64.
9. Najafova Z, Tirado-Magallanes R, Subramaniam M, Hossan T, Schmidt G, Nagarajan S, et al. BRD4 localization to lineage-specific enhancers is associated with a distinct transcription factor repertoire. Nucleic Acids Res. 2017;45:127–41. [PubMed: 27651452]
10. Chang H, Liu Y, Xue M, Liu H, Du S, Zhang L, et al. Synergistic action of master transcription factors controls epithelial-to-mesenchymal transition. Nucleic Acids Res. 2016;44:2514–27. [PubMed: 26926107]
11. Zanconato F, Forcato M, Battilana G, Azzolin L, Quaranta E, Bodega B, et al. Genome-wide association between YAP/TAZ/TEAD and AP-1 at enhancers drives oncogenic growth. Nat Cell Biol. 2015;17:1218–27. [PubMed: 26258633]
12. Liu X, Li H, Rajurkar M, Li Q, Cotton JL, Ou J, et al. Tead and AP1 Coordinate Transcription and Motility. Cell Rep. 2016;14:1169–80. [PubMed: 26832411]
13. Vierbuchen T, Ling E, Cowley CJ, Couch CH, Wang X, Harmin DA, et al. AP-1 Transcription Factors and the BAF Complex Mediate Signal-Dependent Enhancer Selection. Mol Cell. 2017;68:1067–1082.e12. [PubMed: 29272704]
14. Normanno N, De Luca A, Bianco C, Strizzi L, Mancino M, Maiello MR, et al. Epidermal growth factor receptor (EGFR) signaling in cancer. Gene. 2006;366:2–16. [PubMed: 16377102]
15. Salomon DS, Brandt R, Ciardiello F, Normanno N. Epidermal growth factor-related peptides and their receptors in human malignancies. Crit Rev Oncol Hematol. 1995;19:183–232. [PubMed: 7612182]
16. Maiti GP, Mondal P, Mukherjee N, Ghosh A, Ghosh S, Dey S, et al. Overexpression of EGFR in head and neck squamous cell carcinoma is associated with inactivation of SH3GL2 and CDC25A genes. PLoS One. 2013;8:e63440. [PubMed: 23675485]
17. Shinojima N, Tada K, Shiraishi S, Kamiryo T, Kochi M, Nakamura H, et al. Prognostic value of epidermal growth factor receptor in patients with glioblastoma multiforme. Cancer Res. 2003;63:6962–70. [PubMed: 14583498]
18. Chen H, Li C, Peng X, Zhou Z, Weinstein JN, Liang H, et al. A Pan-Cancer Analysis of Enhancer Expression in Nearly 9000 Patient Samples. Cell. 2018;173:386–399.e12. [PubMed: 29625054]
19. Zack TI, Schumacher SE, Carter SL, Cherniack AD, Saksena G, Tabak B, et al. Pan-cancer patterns of somatic copy number alteration. Nat Genet. 2013;45:1134–40. [PubMed: 24071852]
20. Zehir A, Benayed R, Shah RH, Syed A, Middha S, Kim HR, et al. Mutational landscape of metastatic cancer revealed from prospective clinical sequencing of 10,000 patients. Nat Med. 2017;23:703–13. [PubMed: 28481359]
21. Brandt B, Meyer-Staeckling S, Schmidt H, Agelopoulos K, Buerger H. Mechanisms of egfr gene transcription modulation: relationship to cancer risk and therapy response. Clin Cancer Res. 2006;12:7252–60. [PubMed: 17189396]
22. Chrysogelos SA. Chromatin structure of the EGFR gene suggests a role for intron 1 sequences in its regulation in breast cancer cells. Nucleic Acids Res. 1993;21:5736–41. [PubMed: 8284222]
23. Maekawa T, Imamoto F, Merlino GT, Pastan I, Ishii S. Cooperative function of two separate enhancers of the human epidermal growth factor receptor proto-oncogene. J Biol Chem. 1989;264:5488–94. [PubMed: 2925616]

24. Mack SC, Singh I, Wang X, Hirsch R, Wu Q, Villagomez R, et al. Chromatin landscapes reveal developmentally encoded transcriptional states that define human glioblastoma. J Exp Med. 2019;216:1071–90. [PubMed: 30948495]
25. Loo JX, Zhao M, Xia S, Li F, Ke H, He C, et al. E6 Protein Expressed by High-Risk HPV Activates Super-Enhancers of the EGFR and c-MET Oncogenes by Destabilizing the Histone Demethylase KDM5C . Cancer Res. 2018;78:1418–30. [PubMed: 29339538]
26. Gimple RC, Kidwell RL, Kim LJY, Sun T, Gromovsky AD, Wu Q, et al. Glioma Stem Cell Specific Super Enhancer Promotes Polyunsaturated Fatty Acid Synthesis to Support EGFR Signaling. Cancer Discov. 2019;CD-19-0061.
27. Hagège H, Klous P, Braem C, Splinter E, Dekker J, Cathala G, et al. Quantitative analysis of chromosome conformation capture assays (3C-qPCR). Nat Protoc. Nature Publishing Group; 2007;2:1722–33.
28. Li Z, Van Calcar S, Qu C, Cavenee WK, Zhang MQ, Ren B. A global transcriptional regulatory role for c-Myc in Burkitt's lymphoma cells. Proc Natl Acad Sci U S A. National Academy of Sciences; 2003;100:8164–9.
29. Buenrostro JD, Giresi PG, Zaba LC, Chang HY, Greenleaf WJ. Transposition of native chromatin for fast and sensitive epigenomic profiling of open chromatin, DNA-binding proteins and nucleosome position. Nat Methods. 2013;10:1213–8. [PubMed: 24097267]
30. Hnisz D, Abraham BJ, Lee TI, Lau A, Saint-André V, Sigova AA, et al. Super-enhancers in the control of cell identity and disease. Cell. 2013;155:934–47. [PubMed: 24119843]
31. Whyte W a, Orlando D a, Hnisz D, Abraham BJ, Lin CY, Kagey MH, et al. Master transcription factors and mediator establish super-enhancers at key cell identity genes. Cell. 2013;153:307–19. [PubMed: 23582322]
32. Moorthy SD, Davidson S, Shchuka VM, Singh G, Malek-Gilani N, Langroudi L, et al. Enhancers and super-enhancers have an equivalent regulatory role in embryonic stem cells through regulation of single or multiple genes. Genome Res. 2017;27:246–58. [PubMed: 27895109]
33. O'Geen H, Ren C, Nicolet CM, Perez AA, Halmai J, Le VM, et al. dCas9-based epigenome editing suggests acquisition of histone methylation is not sufficient for target gene repression. Nucleic Acids Res. 2017;45:9901–16. [PubMed: 28973434]
34. Gilbert LA, Larson MH, Morsut L, Liu Z, Brar GA, Torres SE, et al. CRISPR-mediated modular RNA-guided regulation of transcription in eukaryotes. Cell. 2013;154:442–51. [PubMed: 23849981]
35. O'Shea EK, Rutkowski R, Kim PS. Mechanism of specificity in the Fos-Jun oncoprotein heterodimer. Cell. 1992;68:699–708. [PubMed: 1739975]
36. Wang ZY, Sato H, Kusam S, Sehra S, Toney LM, Dent AL. Regulation of IL-10 gene expression in Th2 cells by Jun proteins. J Immunol. 2005;174:2098–105. [PubMed: 15699140]
37. Angel P, Hattori K, Smeal T, Karin M. The jun proto-oncogene is positively autoregulated by its product, Jun/AP-1. Cell. 1988;55:875–85. [PubMed: 3142689]
38. Zanca C, Villa GR, Benitez JA, Thorne AH, Koga T, D'Antonio M, et al. Glioblastoma cellular cross-talk converges on NF-κB to attenuate EGFR inhibitor sensitivity. Genes Dev. 2017;31:1212–27. [PubMed: 28724615]
39. LeRoy G, Rickards B, Flint SJ. The Double Bromodomain Proteins Brd2 and Brd3 Couple Histone Acetylation to Transcription. Mol Cell. 2008;30:51–60. [PubMed: 18406326]
40. Filippakopoulos P, Qi J, Picaud S, Shen Y, Smith WB, Fedorov O, et al. Selective inhibition of BET bromodomains. Nature. 2010;468:1067–73. [PubMed: 20871596]
41. Chen Y, Xu L, Mayakonda A, Huang M-L, Kanojia D, Tan TZ, et al. Bromodomain and extraterminal proteins foster the core transcriptional regulatory programs and confer vulnerability in liposarcoma. Nat Commun. 2019;10:1353. [PubMed: 30903020]
42. Tang Z, Li C, Kang B, Gao G, Li C, Zhang Z. GEPIA: a web server for cancer and normal gene expression profiling and interactive analyses. Nucleic Acids Res. 2017;45:W98–102. [PubMed: 28407145]
43. Erjala K, Sundvall M, Junttila TT, Zhang N, Savisalo M, Mali P, et al. Signaling via ErbB2 and ErbB3 associates with resistance and epidermal growth factor receptor (EGFR) amplification with

sensitivity to EGFR inhibitor gefitinib in head and neck squamous cell carcinoma cells. Clin Cancer Res. 2006;12:4103–11. [PubMed: 16818711]

44. Loeffler-Ragg J, Witsch-Baumgartner M, Tzankov A, Hilbe W, Schwentner I, Sprinzl GM, et al. Low incidence of mutations in EGFR kinase domain in Caucasian patients with head and neck squamous cell carcinoma. Eur J Cancer. 2006;42:109–11. [PubMed: 16324836]
45. Patel A, Tirosh I, Trombetta J. Single-cell RNA-seq highlights intratumoral heterogeneity in primary glioblastoma. Science (80-). 2014;1–9.
46. Nathanson D a, Gini B, Mottahedeh J, Visnyei K, Koga T, Gomez G, et al. Targeted therapy resistance mediated by dynamic regulation of extrachromosomal mutant EGFR DNA. Science. 2014;343:72–6. [PubMed: 24310612]
47. Mellinghoff IK, Wang MY, Vivanco I, Haas-Kogan DA, Zhu S, Dia EQ, et al. Molecular Determinants of the Response of Glioblastomas to EGFR Kinase Inhibitors. N Engl J Med. 2005;353:2012–24. [PubMed: 16282176]
48. Yu HA, Arcila ME, Rekhtman N, Sima CS, Zakowski MF, Pao W, et al. Analysis of tumor specimens at the time of acquired resistance to EGFR-TKI therapy in 155 patients with EGFR-mutant lung cancers. Clin Cancer Res. 2013;19:2240–7. [PubMed: 23470965]
49. Thress KS, Paweletz CP, Felip E, Cho BC, Stetson D, Dougherty B, et al. Acquired EGFR C797S mutation mediates resistance to AZD9291 in non-small cell lung cancer harboring EGFR T790M. Nat Med. 2015;21:560–2. [PubMed: 25939061]
50. Yochum ZA, Cades J, Wang H, Chatterjee S, Simons BW, O'Brien JP, et al. Targeting the EMT transcription factor TWIST1 overcomes resistance to EGFR inhibitors in EGFR-mutant non-small-cell lung cancer. Oncogene. 2019;38:656–70. [PubMed: 30171258]
51. Brennan CW, Verhaak RG, McKenna A, Campos B, Noushmehr H, Salama SR, et al. The somatic genomic landscape of glioblastoma. Cell. 2013;155:462–77. [PubMed: 24120142]
52. Takeda DY, Spisák S, Seo J-H, Bell C, O'Connor E, Korthauer K, et al. A Somatically Acquired Enhancer of the Androgen Receptor Is a Noncoding Driver in Advanced Prostate Cancer. Cell. Cell Press; 2018;174:422–432.e13.
53. Zhang X, Choi PS, Francis JM, Imielinski M, Watanabe H, Cherniack AD, et al. Identification of focally amplified lineage-specific super-enhancers in human epithelial cancers. Nat Genet. 2016;48:176–82. [PubMed: 26656844]
54. Huang HS, Nagane M, Klingbeil CK, Lin H, Nishikawa R, Ji XD, et al. The enhanced tumorigenic activity of a mutant epidermal growth factor receptor common in human cancers is mediated by threshold levels of constitutive tyrosine phosphorylation and unattenuated signaling. J Biol Chem. 1997;272:2927–35. [PubMed: 9006938]
55. Jungbluth AA, Stockert E, Huang HJ, Collins VP, Coplan K, Iversen K, et al. A monoclonal antibody recognizing human cancers with amplification/overexpression of the human epidermal growth factor receptor. Proc Natl Acad Sci U S A. 2003;100:639–44. [PubMed: 12515857]
56. Sok JC, Coppelli FM, Thomas SM, Lango MN, Xi S, Hunt JL, et al. Mutant epidermal growth factor receptor (EGFRvIII) contributes to head and neck cancer growth and resistance to EGFR targeting. Clin Cancer Res. 2006;12:5064–73. [PubMed: 16951222]
57. Koga T, Li B, Figueroa JM, Ren B, Chen CC, Carter BS, et al. Mapping of genomic EGFRvIII deletions in glioblastoma: insight into rearrangement mechanisms and biomarker development. Neuro Oncol. 2018;20:1310–20. [PubMed: 29660021]
58. Liu Q, Kulak MV, Borcherding N, Maina PK, Zhang W, Weigel RJ, et al. A novel HER2 gene body enhancer contributes to HER2 expression. Oncogene. 2018;37:687–94. [PubMed: 29035388]
59. Leonard B, Brand TM, O'Keefe RA, Lee ED, Zeng Y, Kemmer JD, et al. BET Inhibition Overcomes Receptor Tyrosine Kinase-Mediated Cetuximab Resistance in HNSCC. Cancer Res. 2018;78:4331–43. [PubMed: 29792310]

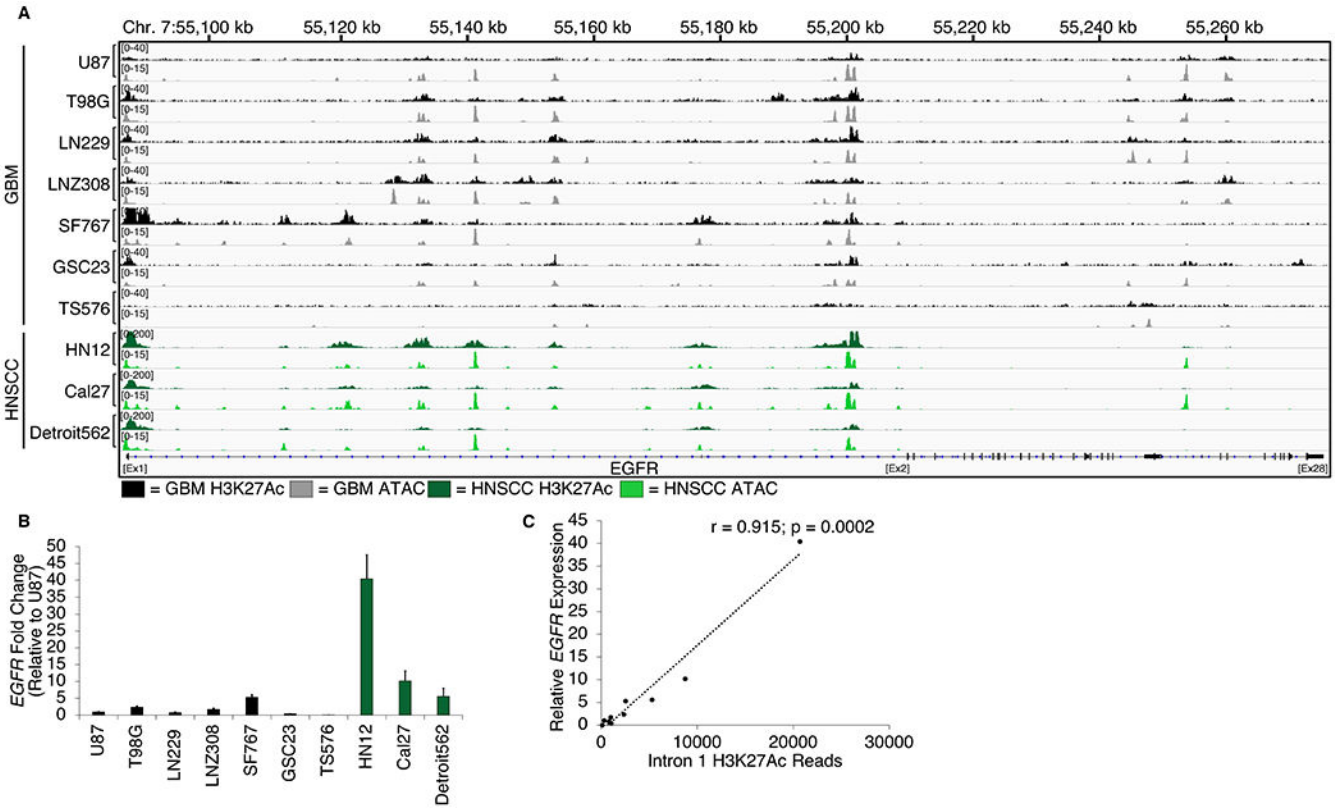

Figure 1.

Chromatin landscape of wild-type EGFR. **A:** IGV snapshots showing H3K27Ac ChIP-seq (dark) and ATAC-seq (light) read densities at the EGFR locus in GBM and HNSCC cell lines. **B:** EGFR expression in 7 GBM and 3 HNSCC cell lines were analyzed by RT-qPCR. EGFR transcript level was first normalized to GAPDH and subsequently calculated as fold change relative to U87. **C.** Total aligned H3K27Ac ChIP-seq reads were calculated and plotted against the relative *EGFR* expression fold change. The relationship was analyzed using Spearman's rank order correlation.

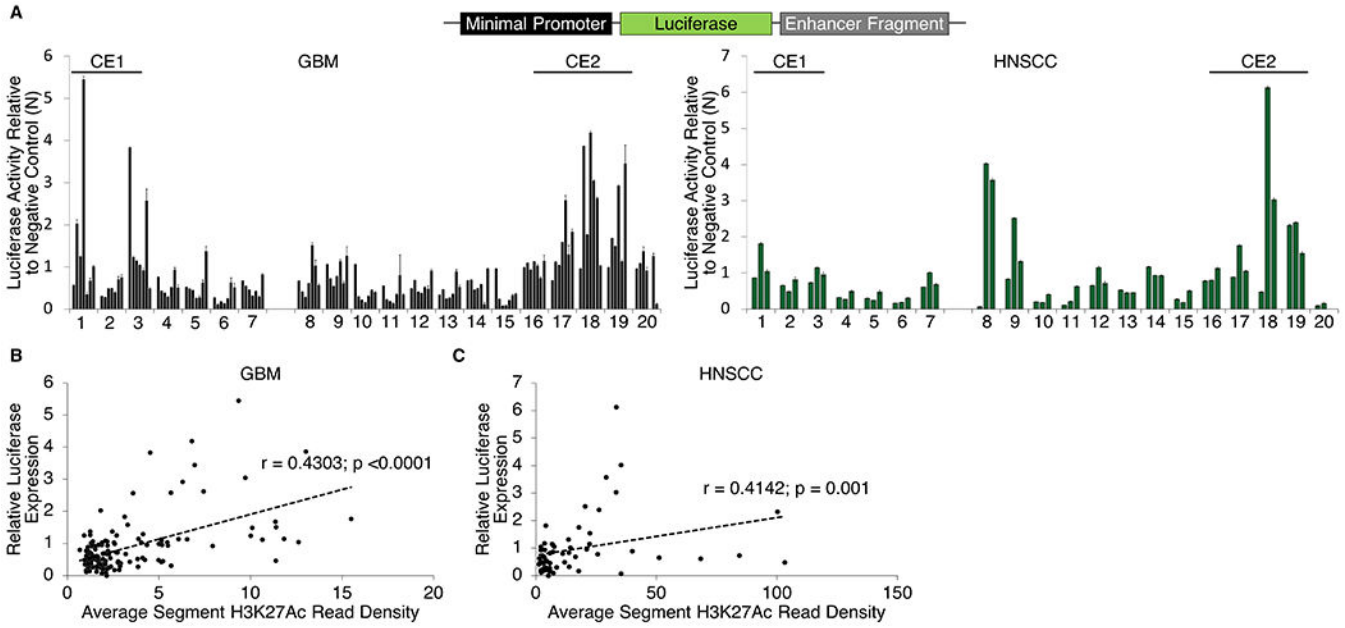

Figure 2.

Identification of critical constituent enhancers in EGFR intron 1. **A:** (Top) Schematic of positioning of the enhancer segments in the pGL4.24 construct. (Bottom) Luciferase activity in GBM (cell lines left to right: U87, T98G, LN229, LNZ308, SF767, GSC23, TS576) and HNSCC (cell lines left to right: HN12, Cal27, Detroit562) cell lines after transfection with pGL4.24 constructs containing cloned fragments of EGFR intron 1. A negative control region 10kb downstream of the EGFR promoter was used for normalization. **B-C:** Relative luciferase expression for P1-20 was plotted against the average H3K27Ac read density for each individual segment in (left) GBM and (right) HNSCC. The relationship was analyzed using Spearman's rank order correlation.

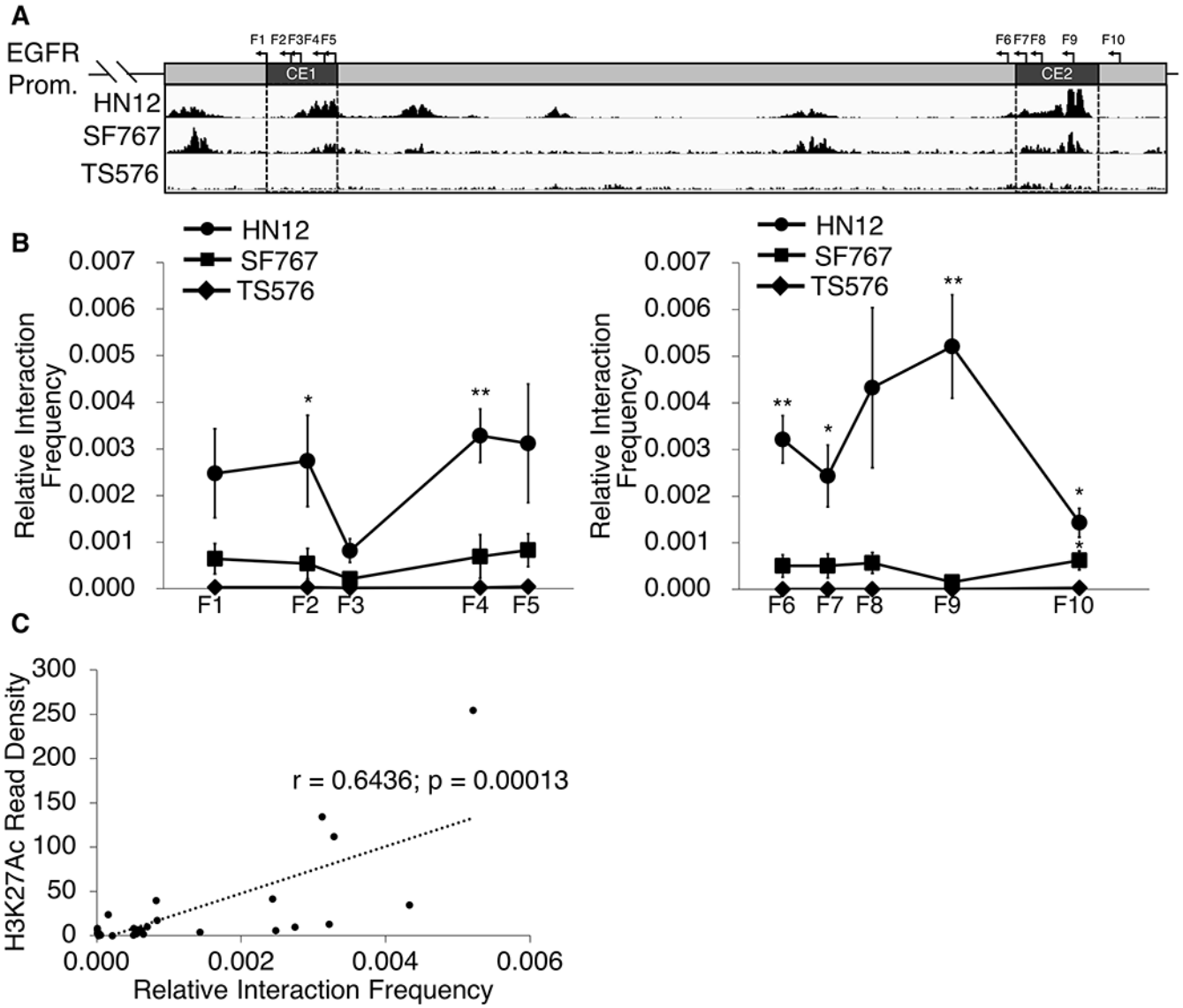

Figure 3.

Enhancer-promoter interaction by chromatin conformation capture (3C). **A:** Schematic showing position of 3C primers relative to CE1 and CE2. 3C qPCR was done in combination with a forward primer in the *EGFR* promoter region. IGV tracks for H3K27Ac in HN12, SF767 and TS576 are shown for reference. **B:** Relative interaction frequency of each restriction fragment (F1-10) was calculated as described in the experimental procedures and was plotted against genomic location of the EcoRI restriction site. Significant differences in interaction are indicated for HN12 relative to control (TS576) (*$p < 0.05$, **$p < 0.005$, n = 3 independent experiments, Student's *t* test). **C:** H3K27Ac read density at the primer site was plotted against the relative interaction frequency for all three measured cell lines. The relationship was analyzed using Spearman's rank order correlation.

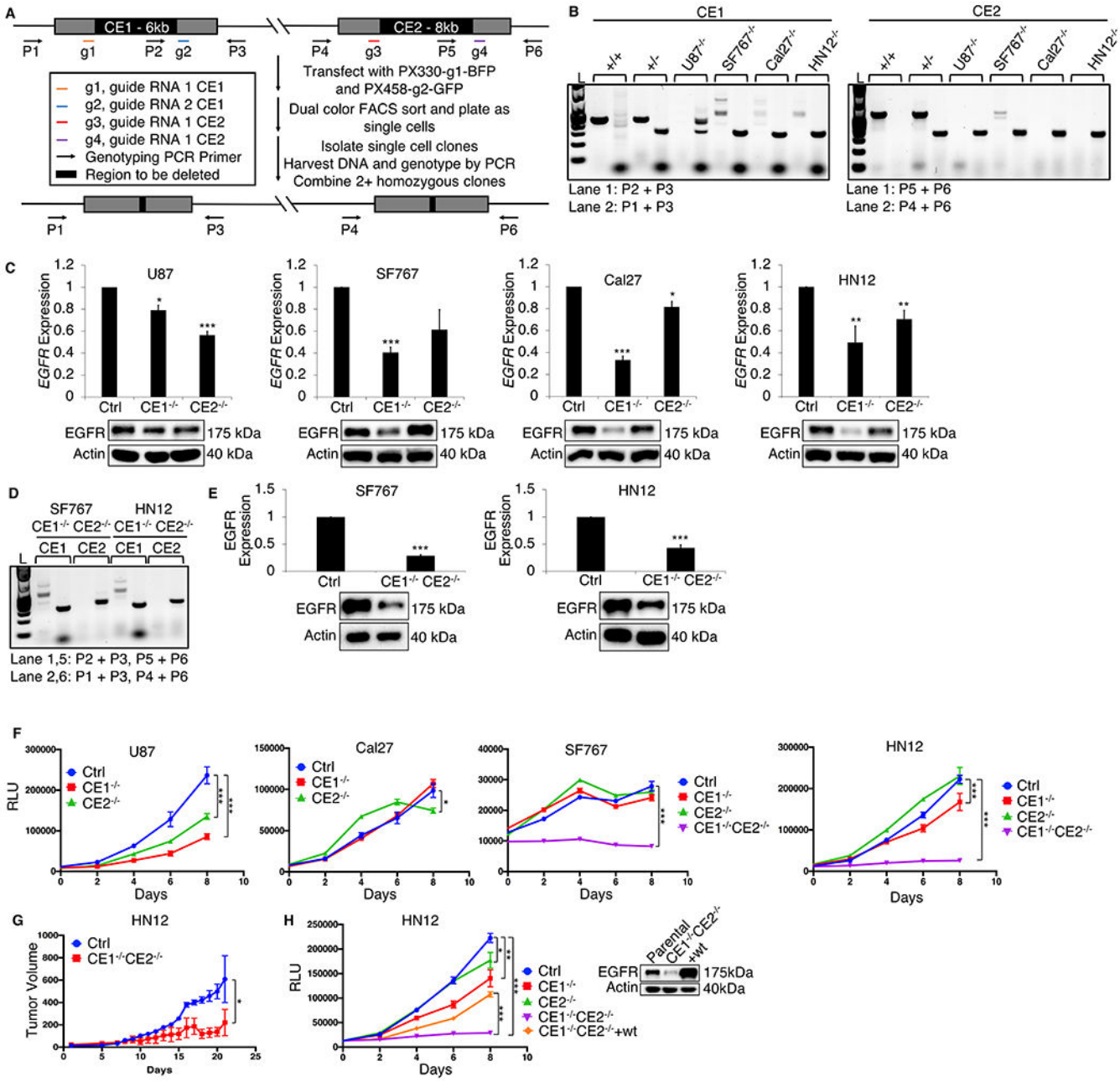

Figure 4.

CRISPR/Cas9-mediated deletion of CE1 and CE2 in GBM and HNSCC cell lines reduces *EGFR* expression and suppresses proliferation. **A:** Schematic outlining the CRISPR/Cas9 deletion strategy. **B:** Genotyping PCR for (left) CE1 and (right) CE2. Homozygous parental (lanes 1, 2) and heterozygous deleted (lanes 3, 4) are shown as PCR controls. Homozygous enhancer deletion (lanes 5-12) is shown for clone mixtures. A minimum of 2 homozygous clones were combined for downstream analysis. **C:** (Top) EGFR expression in deleted cell lines were analyzed by RT-qPCR. *EGFR* transcript level was first normalized to *GAPDH* and subsequently calculated as fold change relative to parental. **D:** Genotyping PCR confirms presence of both deletions in clone mixtures. A minimum of 2 double-deleted

homozygous clones were combined for downstream analysis. **E:** *EGFR* expression in double-deleted cell lines was analyzed by RT-qPCR. *EGFR* transcript level was first normalized to *GAPDH* and subsequently calculated as fold change relative to parental (Ctrl). **F:** Cell proliferation curves were generated by measuring ATP levels every two days over 9 days. Significance is measured relative to parental (Ctrl). **G:** Subcutaneous tumors were generated and tumor volume was measured over 21 days. n = 5 (Ctrl) 4 ($CE1^{-/-}CE2^{-/-}$) *p < 0.05. Volume was measured with the formula $V = (W^2 \times L)/2$. **H:** Wild-type EGFR expression was rescued in double knockout cells by lentiviral transduction. Proliferation was measured by ATP levels every 2 days over 9 days. Significance is measured relative to parental (Ctrl) for knockout cells and relative to double knockout ($CE1^{-/-}CE2^{-/-}$) for wtEGFR rescued cells. **C,E,H:** Western blot for EGFR expression. β-Actin was used as a loading control. **C,E-F,H:** (*p < 0.05, **p < 0.005, ***p < 0.0005, n = 3 independent experiments, Student's *t* test).

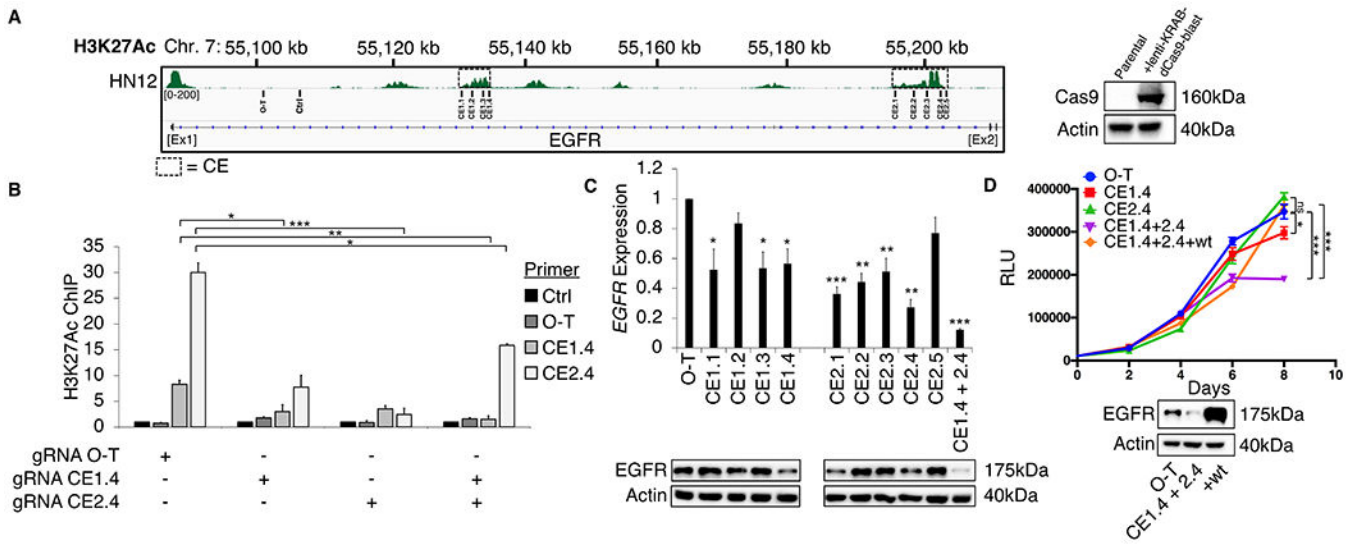

Figure 5.

Targeting dCas9-KRAB to the CE's decreases *EGFR* gene transcription and suppresses proliferation. **A:** (Left) H3K27Ac IGV track of HN12 cells showing the position of gRNA's targeting the *EGFR* intron 1 enhancers and off-target (O-T) control. (Right) Western blot for dCas9-KRAB expression after transduction with lenti-dCas9-KRAB-blast. **B:** H3K27Ac enrichment at the targeted enhancer regions before and after dCas9-KRAB targeting was analyzed by ChIP-qPCR. Primers were designed around the targeted regions as well as a PCR negative control (Ctrl) from a H3K27Ac-negative region within *EGFR* intron 1. **C:** *EGFR* expression in dCas9-KRAB expressing cell lines was analyzed by RT-qPCR. *EGFR* transcript level was first normalized to *GAPDH* and subsequently calculated as fold change relative to off-target control. **D:** Cell proliferation curves were generated by measuring ATP levels every two days over 9 days. Significance is measured relative to O-T for knockdown cells and relative to double knockdown (CE1.4+2.4) for wtEGFR rescued cells. **C-D:** Western blot for EGFR expression. β-Actin was used as a loading control. **B-D:** (*$p < 0.05$, **$p < 0.005$, ***$p < 0.0005$, n = 3 independent experiments, Student's *t* test)

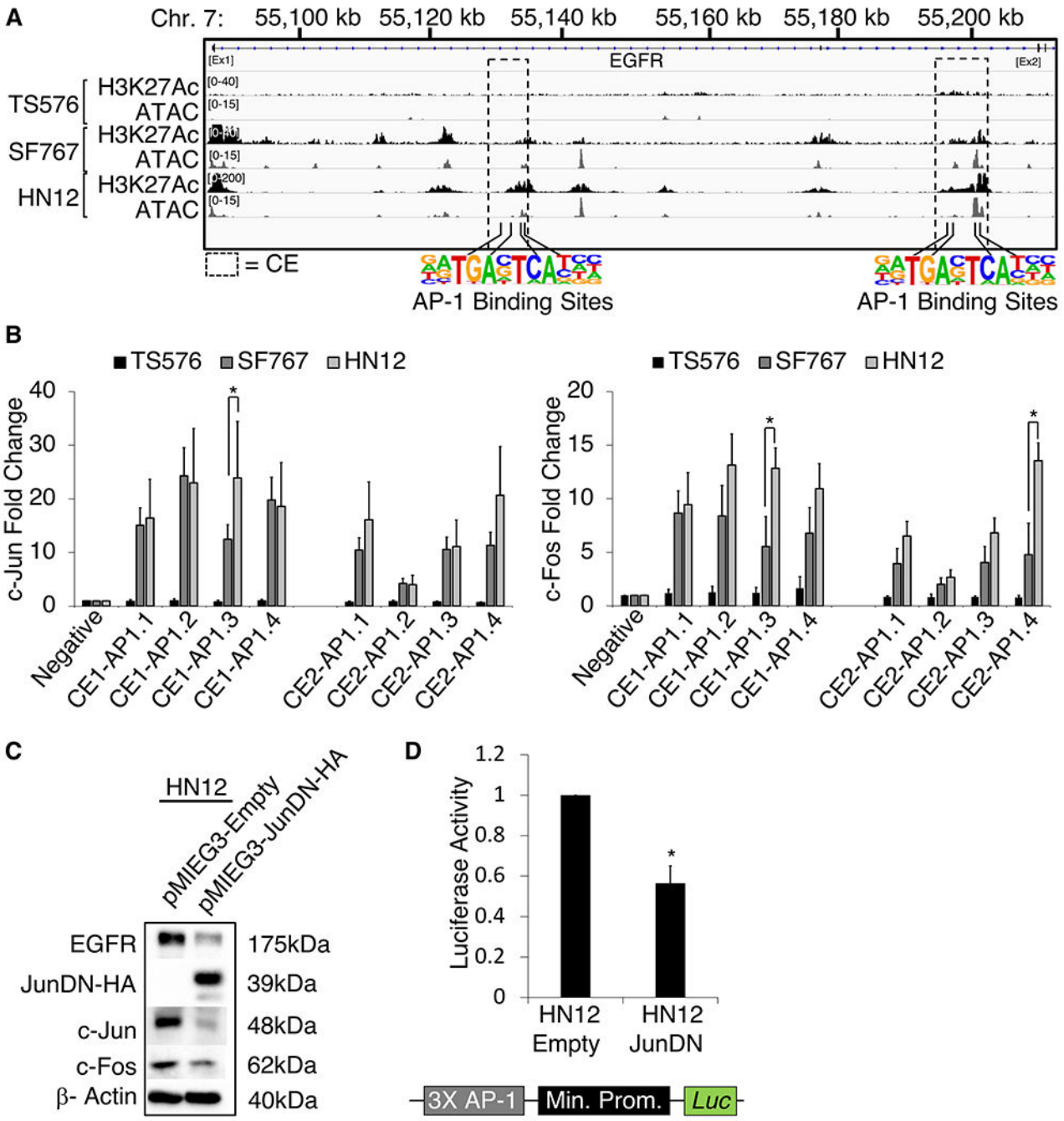

Figure 6.

AP-1 family members bind to and modulate *EGFR* expression. **A:** Schematic of positions of AP-1 binding positions based on ENCODE ChIP-seq data, shown relative to ChIP-seq and ATAC-seq peak density. CE1 and CE2 are highlighted. **B:** Analysis of (left) c-Jun and (right) c-Fos occupancy at the indicated sites. Transcription factor binding is represented as fold change over a negative control region located in chr12. **C:** Analysis of EGFR, JunDN-HA, c-Jun, and c-Fos protein expression in HN12 cells by western blot after transduction with pMIEG3-JunDN-HA. β-Actin was used as a loading control. **D:** Analysis of JunDN efficacy

on a luciferase reporter containing a trimerized AP-1 binding site. **B,D:** (*p < 0.05, **p < 0.005, ***p < 0.0005, n = 3 independent experiments, Student's *t* test)

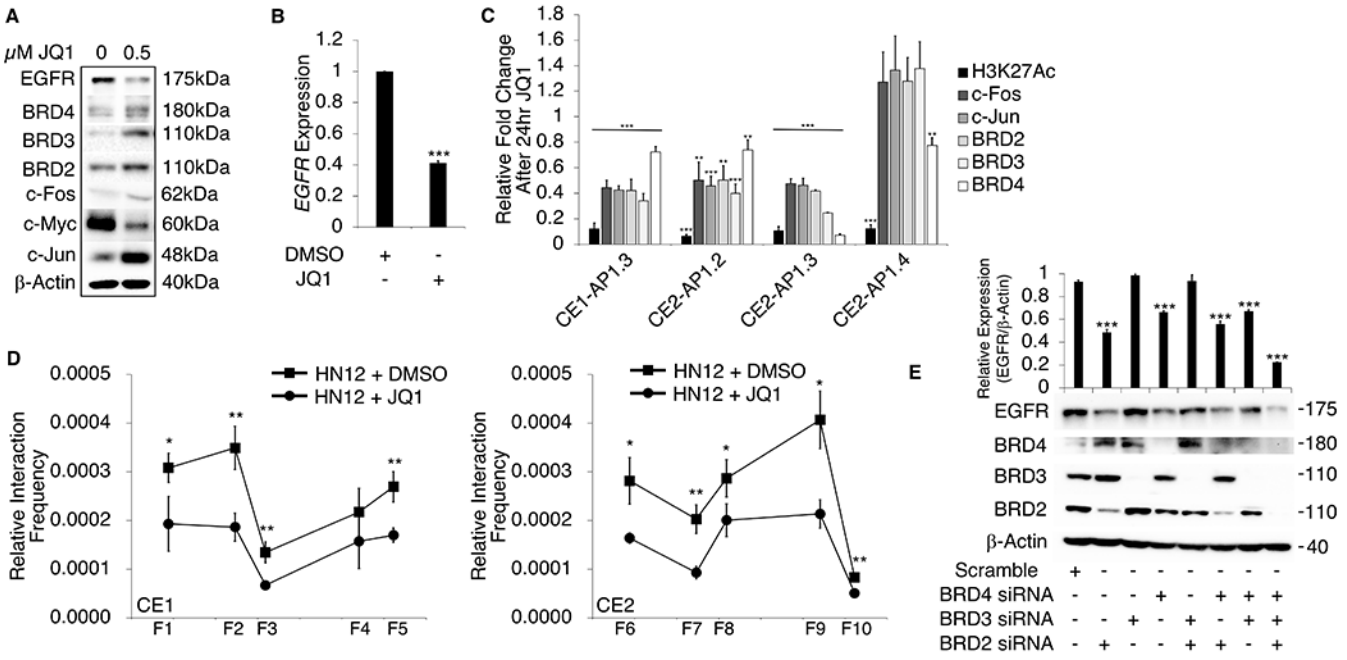

Figure 7.

JQ1 treatment reduces *EGFR* transcription through inhibition of transcription factor activity. **A:** Analysis of EGFR, BRD4, BRD3, BRD2, c-Fos, c-Myc, and c-Jun protein expression in HN12 cells by western blot after treatment with 0.5μM JQ1 for 24 hours. β-Actin was used as a loading control. **B:** *EGFR* expression was analyzed by RT-qPCR in HN12 cells treated with 0.5μM JQ1 for 24 hours. *EGFR* transcript level was first normalized to *GAPDH* and subsequently calculated as fold change relative to DMSO control. **C:** Fold changes in enrichment of the indicated factors after 24 hours of 0.5μM JQ1 was measured at the indicated regions by ChIP-qPCR. ChIP enrichment is normalized to a negative control region in chr12. **D:** Relative interaction frequency by 3C of each restriction fragment (F1-10) was calculated as described in the experimental procedures and was plotted against genomic location of the EcoRI restriction site. Significant differences in interaction are indicated for HN12 +JQ1 relative to control (HN12 +DMSO). **E:** (Bottom) Analysis of EGFR, BRD4, BRD3, BRD2 and β-Actin protein expression in HN12 cells by western blot after treatment with indicated siRNA. A scrambled siRNA was used as treatment control and β-Actin was used as a loading control. (Top) Quantification of relative protein expression. Significance is measured relative to scramble control. **B-E:** (*$p < 0.05$, **$p < 0.005$, ***$p < 0.0005$, n = 3 independent experiments, Student's *t* test)